

On Designing the Nowacki's Device Enabling the Analysis of Deformation and Temperature in the Shear Zone

Bartosz ŁUCZAK

*Poznan University of Technology, Institute of Structural Engineering,
bartosz.luczak@put.poznan.pl*

Wojciech SUMELKA

*Poznan University of Technology, Institute of Structural Engineering,
wojciech.sumelka@put.poznan.pl*

Tomasz ŁODYGOWSKI

*Poznan University of Technology, Institute of Structural Engineering,
tomasz.lodygowski@put.poznan.pl*

Abstract

In this paper a general scheme and designing challenges encountered during design of Nowacki's shear device are presented. The novelty of the approach shown is combining 3D modelling of the whole experimental stand in Catia software with FEM simulations in Abaqus. Linking these two applications allow updating of the model effectively based on feedback from FEM analysis.

Keywords: Nowacki's shear device, FEM simulation, 3D modelling, design experimental equipment

1. Introduction

Nowadays a good knowledge about materials strength and their properties in extreme conditions are key points in designing better and more durable products. At the same time obtaining such parameters requires more complex and more subtle research methods. One of these types of analyses is Nowacki's shear test which allows to determine the material properties under a wide range of strain rates and temperature ranges [3, 12]. However, this demanding test requires a special device which has to withstand extremely difficult working conditions as well as a full insight into the deformation and the temperatures. This paper is one of the few studies to presents a process of designing this laboratory equipment, showing problems encountered.

2. High strain shear test

The first work proposing the concept of shear test at high strain rates was by G'Sell [1]. Originally it was dedicated to polymers, later it was adapted for testing steel sheets. The Nowacki's method is one of modifications of the testing scheme originally proposed by Yoshida and Myauchi [10] in which the specimen has two symmetrically placed zones of shear – the scheme is presented in Figure 1.

Other works on pure shear tests by Guélin [4], Tourbai et al. [9] introduce very rigid frame construction shear device in which only plane pure shear occurs with no lateral

force. For the high-speed loadings it is better and more convenient to use the split Hopkinson pressure bar (SHPB). However, the standard SHPB method has some limitations and results obtained are difficult to interpret properly [6]. To eliminate these disadvantages Gary and Nowacki [2] developed new shear device which consists of two coaxial parts - external frame and cylindrical internal part acting as a clamp in which a specimen is mounted. The general scheme of the device is shown in Figure 2.

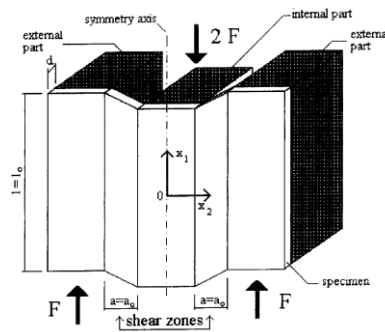


Figure 1. Testing scheme with two zones of shear [6]

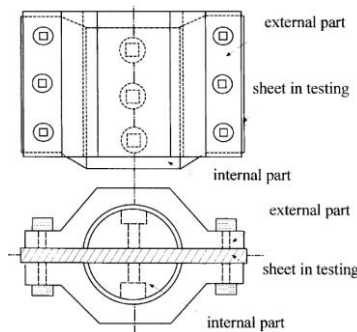


Figure 2. Device for high strain shear test [2]

The next important improvement of high shear test was the introduction of the direct impact method by Klepaczko [5]. It allowed to extend the studies of the dynamic plastic limit of metal sheets. This new method had allowed higher strain rates in the specimen compared to the standard split Hopkinson pressure bar. The new direct impact configuration, in which flat projectile hit's directly in device placed in front of the transmitter tube, prevents the formation of a wave reflections from interference, which was one of disadvantages of SHPB method. Experiential configurations for both direct impact and standard SHPB methods are shown in Figure 3.

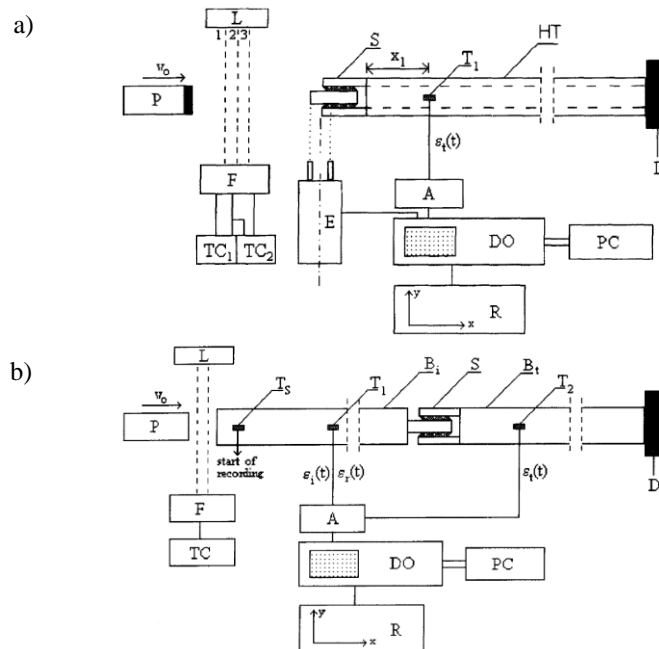


Figure 3. Experimental configurations: a) direct impact, b) standard SHPB. P – projectile, Bi – incident bar, Bt – transmitter bar, S – shear device with double shear specimen, HT – Hopkinson tube, D – damper [5]

3. Designing Nowacki’s device – general scheme

In this paper we discuss in general terms the way of designing the Nowacki’s device and we focus on the problems which have occurred during analysis. The key features are full insight into the deformation and the temperatures in the shear zones. The first step in the designing process of the shear device was preparing 3D geometrical model of the whole experimental stand which would be appropriate for the gas gun available in laboratory of Poznan University of Technology.



Figure 4. Existing gas gun

Geometry was built up on sketches, photographs and measurements collected from the existing device, and support structure. The entire 3D model, which consisted of nine individual elements was created in CAM/CAD software the Catia V5, because this application gives the best integration with FEM analysis software Abaqus - which was used later to analyse the strength and the behaviour of the device under different strikes velocities (direct impact configuration). Catia V5 additionally allows to combine all elements into single part to check and ensure that any collisions do not occur. Finally its functions were used to prepare 2D technical drawings for manufacturing. The prepared 3D model is presented in Figure 5.

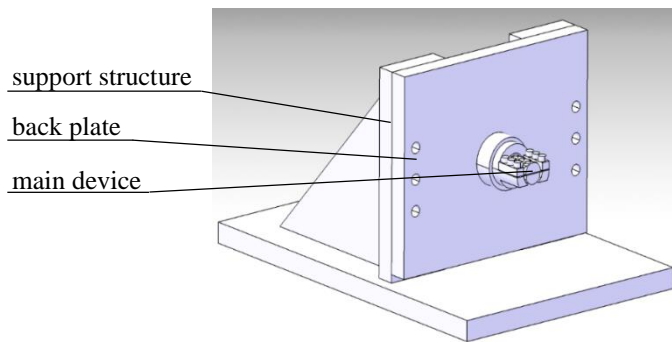


Figure 5. Entire model assembled in Catia V5

Next some simplifications were made to prepare model for the FEM analysis. After geometry import into the Abaqus, materials definitions were added and assigned to elements - single parts were connected and boundary conditions were added.

Two material models were used in the analyses: perfectly elastic-plastic for elements of the device; and the second the Johnson-Cook (JC) model with hardening and damage evolution for specimen [7, 11]. In the model three different materials can be distinguished: aluminium which is the specimen made from; high-strength cold work tool steel NC6 which is used for all the elements of the device; and S235JR steel for all bolts. Material parameters are presented in Tables 1-3. It should be emphasised that the material parameters in Table 1 describe the evolution of yield stress in JC model denoted by σ_y (middle column)

$$\sigma_y = [A + B(\epsilon^{-pl})^n] \left[1 + C \ln \left(\frac{\dot{\epsilon}}{\dot{\epsilon}_0} \right) \right] (1 - \hat{\vartheta}^m), \quad (1)$$

where

$$\hat{\vartheta} \equiv \begin{cases} 0 & \text{for } \vartheta < \vartheta_{transition} \\ (\vartheta - \vartheta_{transition}) / (\vartheta_{melt} - \vartheta_{transition}) & \text{for } \vartheta_{transition} \leq \vartheta \leq \vartheta_{melt} \\ 1 & \text{for } \vartheta > \vartheta_{melt} \end{cases}, \quad (2)$$

and (last column) the evolution equivalent failure plastic strain $\bar{\epsilon}_D^{pl}$ (therefore the fracture energy for damage evolution was set to $G_f = 0.0$).

$$\bar{\epsilon}_D^{pl} = [d_1 + d_2 \exp(-d_3 \eta)] \left[1 + d_4 \ln \left(\frac{\dot{\epsilon}^{pl}}{\dot{\epsilon}_0} \right) \right] (1 + d_5 \hat{\theta}). \quad (3)$$

Other parameters denote: ρ is the density, E is the Young's modulus and ν is the Poisson ratio.

Table 1. Material properties for aluminium

$\rho = 2700 \text{ kg/m}^3$	$A = 324.0 \text{ MPa}$	$d_1 = -0.77$
$E = 200 \text{ GPa}$	$B = 113.0 \text{ MPa}$	$d_2 = 1.45$
$\nu = 0.30$	$n = 0.42$	$d_3 = 0.47$
	$m = 1.34$	$d_4 = 0.0$
	$\theta_{melt} = 925.0 \text{ K}$	$d_5 = 1.60$
	$\theta_{transition} = 293.2 \text{ K}$	$\dot{\epsilon}^{pl} = 1.0$
	$C = 0.002$	$G_f = 0.0$
	$\dot{\epsilon}_0 = 1.0$	

Table 2. Material properties for NC6 steel

$\rho = 7850 \text{ kg/m}^3$
$E = 200 \text{ GPa}$
$\nu = 0.30$
$\sigma_y = 927 \text{ MPa}$

Table 3. Material properties for steel S235

$\rho = 7850 \text{ kg/m}^3$
$E = 210 \text{ GPa}$
$\nu = 0.27$
$\sigma_y = 450 \text{ MPa}$

The boundary conditions were applied to the support structure, and whole bottom surface was assumed as fully fixed. Other parts were connected to each other by "tie" constraint. Simulations were performed in Abaqus Explicit software which is intended to use for extreme dynamic analyses.

The analysis was performed for different bullet velocities starting with velocity $v = 25 \text{ m/s}$ to maximum striker velocity $v = 300 \text{ m/s}$, simulation time was depended on velocity assumed in analysis and it ranged from to 0.0012 to 0.00010 s. The stable time increment for this time range was between $2.3 \cdot 10^{-9}$ to $2.9 \cdot 10^{-9}$.

Device parts were meshed using finite elements C3D8R (8-node linear brick, reduced integration element). The approximate global size of element is in the range of 0.25 mm

for specimen to 12 mm for support structure. The mesh is not uniform for all elements, its finest depends on the shape and the importance of part (in the sense of expected high strain gradients).

4. Designing process

The aim of the design from the beginning was to obtain the highest possible stiffness of device to ensure that experimental measurements will be unaffected by the stability of the whole test stand. Simulations also allowed to determine the "safe" velocity limitations – maximum projectile velocity which does not destroy the test device.

To meet the above mentioned goal in the simulation the whole model together with existing support structure were taken into account. The first part, which is simple element but is most important for obtaining good results is the back plate.

In the first version the back plate was 10 mm thick and to get maximum stiffness the stiffening ribs were added but following analyses and due to possible problems in the production of the element this design assumptions was changed. Next version was a 20 mm thick plate and the stiffening ribs were removed - further simulations proved that this geometry is stable and rigid enough.

The main part of the device is the most complex and requires very high precision in the manufacturing and strength. The key part of this element are "tables" on both sides to carry the specimen in the fixed position. On their surface small "teeth" 2 mm long, 1 mm wide and 0.5 mm height are prepared to "bite into" steel specimen. Each of "tables" has three $D = 4$ mm diameter thread holes to accommodate bolts that will provide regular compression specimen to the "teeth" and other parts. Because of the shape of this part and complexity of problem how the "teeth" work the model was simplified, the small teeth were removed, the outside thread and those "teeth" were replaced by Abaqus "tie" constraint. However replacing the "teeth" by the tie connection caused a problem with a mesh during the analyses. The finite elements were disappearing or were moving in odd way in all directions, that effect could be observed especially at high striker velocities. In the next version the "tie" connection was applied only on the surfaces where in the real device thread occurs – outside surface of bolts and inside surfaces of holes in main part. The model prepared in Catia V5 and simplified part model are shown in Figure 6.

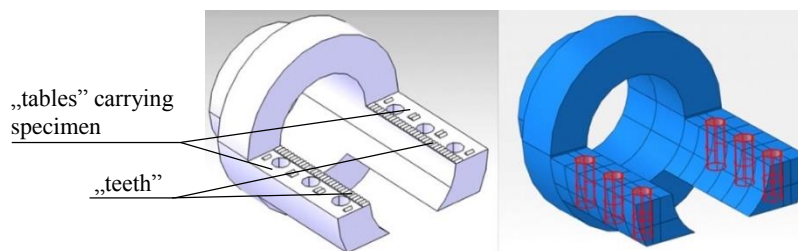


Figure 6. Main part model from Catia V5 (left), from Abaqus with highlighted "tie" constraint area (right)

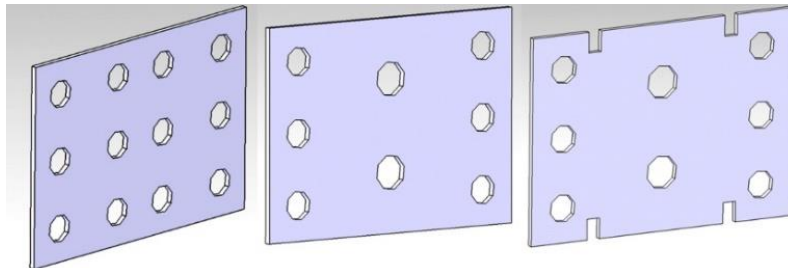


Figure 7. Specimen comparison - 1st iteration (left), 2nd iteration (centre), 3rd iteration (right)

The specimen sizes and the shape were dictated by other parts of device, only its thickness was restricted by the testing method. The maximum thickness of the specimen was assumed 0.80 mm which is a thickness for which when the bullet strikes causes only shear forces. After a series of analyses it turned out that for the high velocity of the striker energy required to shear the specimen is greater than energy required to plasticize the device which resulted in the destruction of the part of the device during the test. The geometry of sheet was changed - two middle rows of six bolts were replaced by only two bigger bolts but the re-designing the part didn't solve the problem of destroying device during the higher velocity strikes. The shape was remodelled again - four notches were added, two per each end of sheet it was made to localize the shear zones and that solved the problem. Comparison of these three iterations is shown in Figure 7.

Connection between the specimen and other part of device was causing trouble due to very difficult and complicated problem of how the device works in reality. In the first analyses this connection was realized as an Abaqus "tie" constraint, the top and bottom areas of specimen were tied with corresponding areas on other parts. Nevertheless analysis showed that the "tie" constraint was inappropriate for dynamic processes, causing a disappearance of mesh elements and odd point movements - which could distort final results - both problems mentioned are shown in Figure 8.

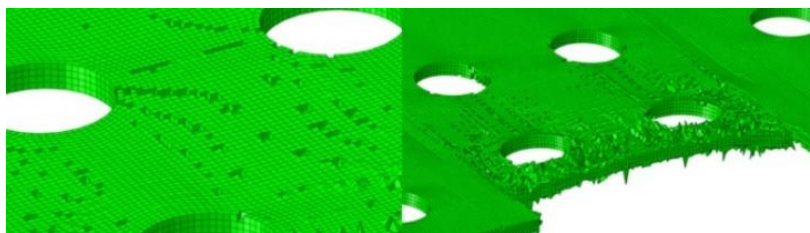


Figure 8. Specimen problems during high strain simulations

At the next stages "tie" constraint was removed, connection was obtained by the tension strength of bolts and general contact with small coefficient friction equal to value of coefficient friction for steel to steel connection ($\mu = 0.3$), which doesn't allow the

specimen to slip from device. However this low value of friction coefficient resulted that shears zones moved closer to bolts, outside of the initially assumed areas – these issues are shown in Figure 9. Finally the friction coefficient was set at 0.999, which partially solved the problem.

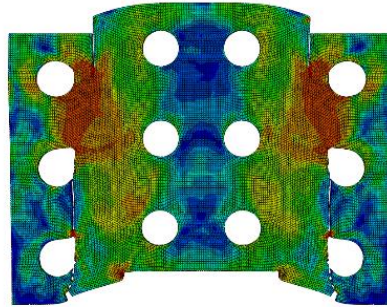


Figure 9. Shifted shear zones

The most homogenous shear zone were obtained for first model with “tie” constrain on the surface between the specimen and the half-cylinders. Nevertheless this solution caused a problem with the mesh that can be observed in Figure 10. The compromise between the homogeneity of shear zones (which is fundamental for material parameters identification) and good mesh quality was the third model with notches which help to localize the shear zones during the test. In reality the “teeth” which are on the surfaces of the half-cylinders will provide strong connection and together with notches will allow to obtain homogenous shear zones.

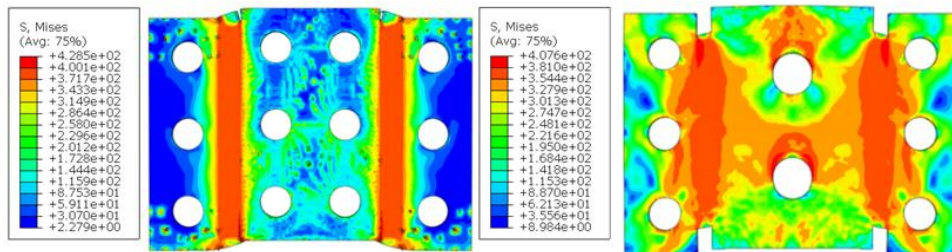


Figure 10. Comparison von Mises stresses for specimens - 1st iteration (left), final iteration (right)

The most difficult part to design in this project were two middle cylindrical parts shown in Figure 11 which have to resist the impact of the striker during the tests and then transfer load from hit to shear forces on specimen. The sizes and complicated form of this piece generated difficulties during modelling and then in the analyses.

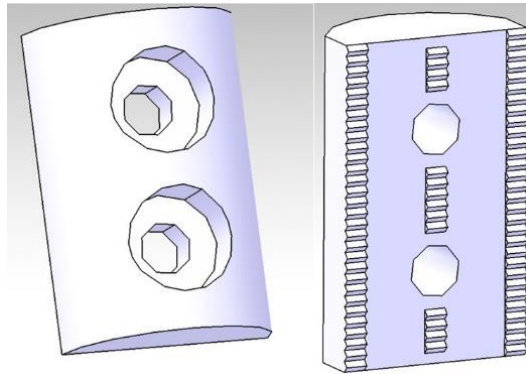


Figure 11. Cylindrical parts - top (left), bottom (right)

The upper half-cylinder at the beginning had six holes $\phi 4$ mm which were counter bored to ensure that the head of bolts would not stick out from the cylinder. All analyses that were run showed that this was the weakest element of the entire device, therefore, because of its importance, to receive valuable results, first the geometry was modified. The original shape with holes for six M4 bolts was replaced by new with only two, bigger M5 bolts. The second version of the design of this part resulted in increasing the striker velocity which didn't destroy the device, however also resulted in a new problem, not observed earlier. Reduction of bolts number contributes to increase the steel section size but also influences the stiffness and bolt connection strength. As a result the bolted part started opening after the striker hit as it is shown in Figure 12.

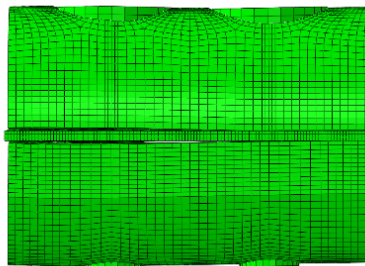


Figure 12. Part opening issue

Designing the bottom half-cylinder proceeded in very similar way to designing upper half-cylinder. The first geometry had to be modified to fit in with the redesigned upper half-cylinder. Other parts not mentioned in the article were designed in similar way.

Eight parts were designed, their final geometry is presented in Figure 13 – Figure 18 which are the technical drawings prepared in Catia V5. The first, a back plate, is presented in Figure 13. This element is made of NC6 steel, and it is connected to a stand with bolts.

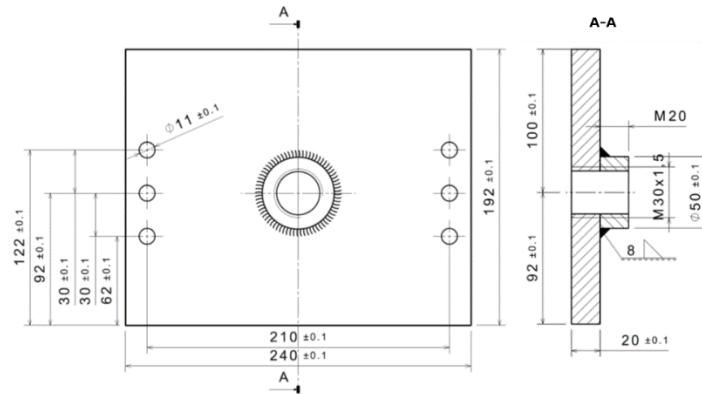


Figure 13. Back plate technical drawing

The main part final geometry is presented in Figure 14. The part is made of high strength steel NC6 and it is connected to back plate using thread connection.

Next, the specimen geometry is shown in Figure 15, the element is made of aluminium.

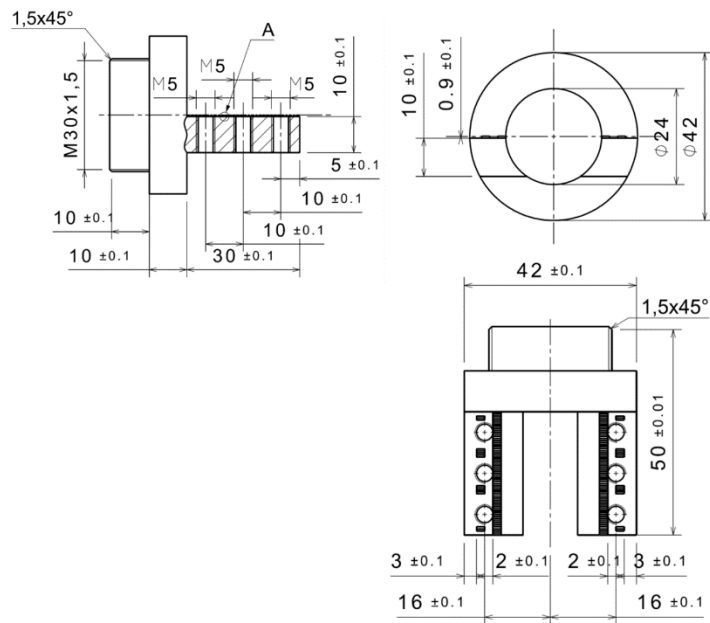


Figure 14. Main part technical drawing

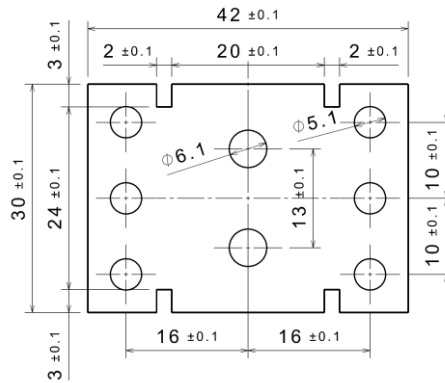


Figure 15. Specimen technical drawing

Upper half-cylinder geometry is shown in Figure 16, and the bottom half-cylinder geometry is presented in Figure 17. The elements are made of NMV steel. They are holding the specimen and in them bolts are hosted.

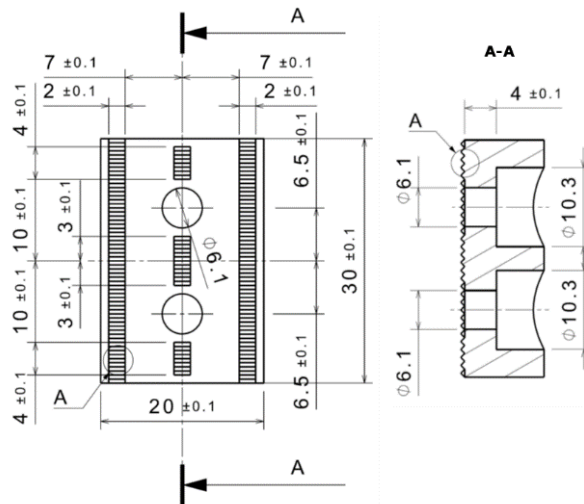


Figure 16. Upper cylinder technical drawing

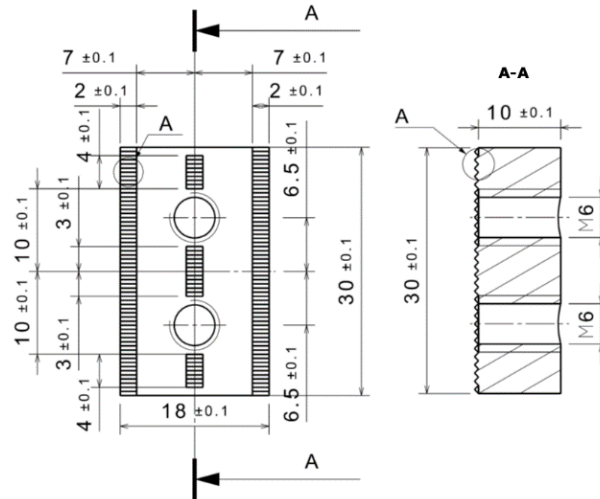


Figure 17. Bottom cylinder technical drawing

The elements which weren't mentioned earlier but which were also designed are the two symmetrical rectangular blocks which are holding the specimen. The geometry of these parts is presented in Figure 18. These rectangular blocks are made of NC6 steel.

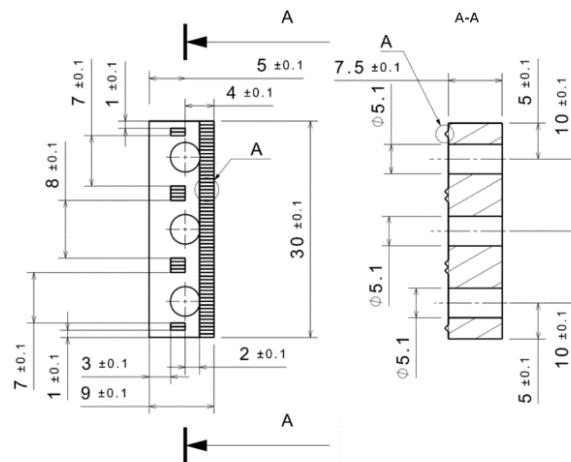


Figure 18. Rectangular block technical drawing

All manufactured elements assembled together are shown in Figure 19.



Figure 19. Manufactured device

5. Conclusions

In this paper the modern concept of designing experimental equipment was presented, an approach combining 3D modelling of the whole experimental stand with FEM simulations. Also crucial problems encountered during designing the device were presented. The obtained results show the impact of the geometry on the strength of the device and the importance of proper modelling contact between the parts. Another important factor which influences the maximum strain rate which can be obtained in the device is the shape of the specimen and the material selected during the design. Additionally, the simulations allowed to determine safe impact velocity for the device, which is important for safety and durability of the equipment. The obtained device together with rigid support ensured the reduction of spurious vibrations, which is fundamental for proper interpretation of obtained measurements i.e. the deformation and the temperature in the shear zone.

References

1. C. G'Sell, S. Boni, S. Shrivastava, *Application of the plane simple shear test for determination of the plastic behaviour of solid polymers at large strains*, J. Mater. Sci., **18**(3) (1983) 903–918.
2. G. Gary, W. K. Nowacki, *Essai de cisaillement plan appliqué à des tôles minces*, Le J. Phys. IV, **4**(C8) (1994) C8-65 – C8-70.
3. A. Glema, T. Łodygowski, W. Sumelka, *Nowacki's double shear test in the framework of the anisotropic thermo-elasto-viscoplastic material model*, J. Theor. Appl. Mech., **48**(4) (2010).
4. P. Guelin, *Comments on Mechanical Hysteresis. Bases of a Thermomechanical Heredity-Structure Scheme.*, J. Mec., **19**(2) (1980) 217 – 247.

5. J. R. Klepaczko, *An experimental technique for shear testing at high and very high strain rates. The case of a mild steel*, Int. J. Impact Eng., 1994.
6. J. R. Klepaczko, H. V. Nguyen, W. K. Nowacki, *Quasi-static and dynamic shearing of sheet metals*, Eur. J. Mech. A/Solids, 1999.
7. J. Litonski, *Plastic flow of a tube under adiabatic torsion*, Acad. Pol. des Sci. Bull. Ser. des Sci. Tech., **25**(1) (1977) 1.
8. B. Luczak, *Master thesis. Design of Support Structure for the Nowacki's Device*, 2015.
9. A. Tourabi, B. Wack, P. Guelin, D. Favier, P. Pegon, W. K. Nowacki, *Remarks on an Experimental Plane Shear Test and on an Anisotropic Elastic-Plastic Theory*, 1993.
10. K. Yoshida, K. Miyauchi, *Experimental Studies of Material Behavior as Related to Sheet Metal Forming*, in *Mechanics of Sheet Metal Forming*, Boston, MA: Springer US, 1978, 19 – 52.
11. M. Szymczyk, W. Sumelka, T. Łodygowski, Numerical investigation on ballistic resistance of aluminium multi-layered panels impacted by improvised projectiles, *Archive of Applied Mechanics*, **88** (2018) 51 – 63.
12. W. Sumelka, Role of Covariance in Continuum Damage Mechanics, *ASCE Journal of Engineering Mechanics*, **139**(11) (2013) 1610 – 1620.